COMPARISON OF OSCILLATORY BEHAVIOR ON InP ELECTRODES IN KOH AND $(NH_4)_2S$

C. O'Dwyer[†‡], T. Melly[†‡], E. Harvey[†‡], D. N. Buckley[†‡], V. J. Cunnane[‡*], D. Sutton[‡], and S. B. Newcomb[‡]

[†] *Dept. of Physics, University of Limerick, Ireland*
[‡] *Materials and Surface Science Institute, University of Limerick, Ireland*
[*] *Dept. of Chemistry and Environmental Science, University of Limerick, Ireland*

ABSTRACT

The observation of current oscillations under potential sweep conditions when an n-InP electrode is anodized in a KOH electrolyte is reported and compared to the oscillatory behavior noted during anodization in an $(NH_4)_2S$ electrolyte. In both cases oscillations are observed above 1.7 V (SCE). The charge per cycle was found to increase linearly with potential for the InP/KOH system but was observed to be independent of potential for the InP/$(NH_4)_2S$ system. The period of the oscillations in the InP/KOH was found to increase with applied potential. In this case the oscillations are asymmetrical and the rising and falling segments have a different dependence on potential. Although the exact mechanism is not yet know for either system, transmission electron microscopy studies show that in both cases, the electrode is covered by a thick porous film in the oscillatory region.

INTRODUCTION

There have been numerous reports of oscillatory behavior during the anodization of semiconductor electrodes in aqueous solution. Similar oscillatory behavior has also been reported for metal anodes under a variety of conditions in many electrode/electrolyte systems [1-6]. Oscillations have been observed during the anodization of p-type [7-10] and n-type [11-13] silicon electrodes mainly in fluoride containing electrolytes. The oscillations are typically observed in the electropolishing region of the applied potential where a thin surface film is present [14]. Evidence for the cyclic growth and dissolution of thin SiO_2 layers on the silicon surface during the oscillatory regime was reported by Parkhutik [15,16]. The shape, frequency and duration of the oscillatory behavior were reported to be dependent on electrolyte composition, temperature, applied anodic current density and crystal orientation of the substrate. Several hypotheses have been proposed, [17,18] but as yet, no general mechanism has been advanced which explains all of the reported results.

Recently, oscillatory behavior has been reported on n-InP electrodes under anodic conditions [19,20]. The oscillatory behavior of InP anodized in $(NH_4)_2S$ was found to be very robust and a constant charge per cycle was reported which was independent of solution pH, $(NH_4)_2S$ concentration and potential scan rate. Thick, porous In_2S_3 films were formed in the oscillatory region of potential. The growth of porous InP layers is also reported when InP electrodes are anodized galvanostatically in HCl and potential oscillations are also observed when the applied current densities are relatively large. These

voltage oscillations have been reported to be linked to the synchronous lateral modulation of the pore diameter during anodization [21].

In this paper, the characteristics of current oscillations observed during the anodization of InP electrodes in KOH are described and contrasted with the behavior observed in $(NH_4)_2S$ electrolytes.

EXPERIMENTAL

The working electrode consisted of polished (100)-oriented monocrystalline sulfur doped n-InP with a carrier concentration of approximately 3×10^{18} cm^{-3}. An ohmic contact was made by alloying indium to the InP sample and the contact was isolated from the electrolyte by means of a suitable varnish. Anodization was carried out in either 5 mol dm^{-3} KOH or 3 mol dm^{-3} $(NH_4)_2S$ electrolytes. A conventional three electrode configuration was used employing a platinum counter electrode and saturated calomel reference electrode (SCE) to which all potentials are referenced. Prior to immersion in the electrolyte, the working electrode was dipped in a 3:1:1 H_2SO_4:H_2O_2:H_2O etchant and rinsed in deionized water. All of the electrochemical experiments were carried out at room temperature and in the dark.

A CH Instruments Model 650A Electrochemical Workstation interfaced to a Personal Computer (PC) was employed for cell parameter control and for data acquisition. Cross-sectional slices were thinned to electron transparency using standard focused ion beam milling procedures by means of a FEI 200 FIBSIMS workstation. The transmission electron microscopy (TEM) characterization was performed using a JEOL 2010 TEM operating at 200 kV.

RESULTS AND DISCUSSION

InP/KOH

Linear potential sweeps were taken at a series of scan rates in the range 50 mV s^{-1} to 500 mV s^{-1} in a 5 mol dm^{-3} aqueous KOH electrolyte. A typical current density vs. potential curve for an n-InP electrode is shown in Fig. 1a. The potential was scanned at a rate of 100 mV s^{-1} from an initial potential of 0.0 V to an upper potential of 2.4 V. The current density measured is small in the potential range 0.0 to 0.5 V. From 0.5 V to 0.8 V a rapid rise in the current density is observed. The current within this potential region is associated with the formation of a porous InP layer [22]. The current density then continues to rise more slowly as the potential is further increased to 1.2 V where a maximum of 0.2 A cm^{-2} in the current density is reached. The current density decreases with further increases in potential up to 1.7 V where it increases abruptly. Well defined current oscillations are observed in the potential range 2.1 V to 2.3 V and have an average current density of 0.35 A cm^{-2}.

The current density vs. potential curves were found to have a similar oscillatory region for all the scan rates investigated. Fig. 1b is the voltammetric response of an n-InP electrode at a scan rate of 400 mV s^{-1}. As is obvious from comparing Fig. 1a and Fig. 1b, increasing the scan rate results in the shifting of the current-voltage response to more

anodic potentials. In Fig. 1b the current oscillations now lie in the potential range 2.9 V to 3.5 V. Furthermore, the average current density of the oscillations is observed to increase with increasing scan rate.

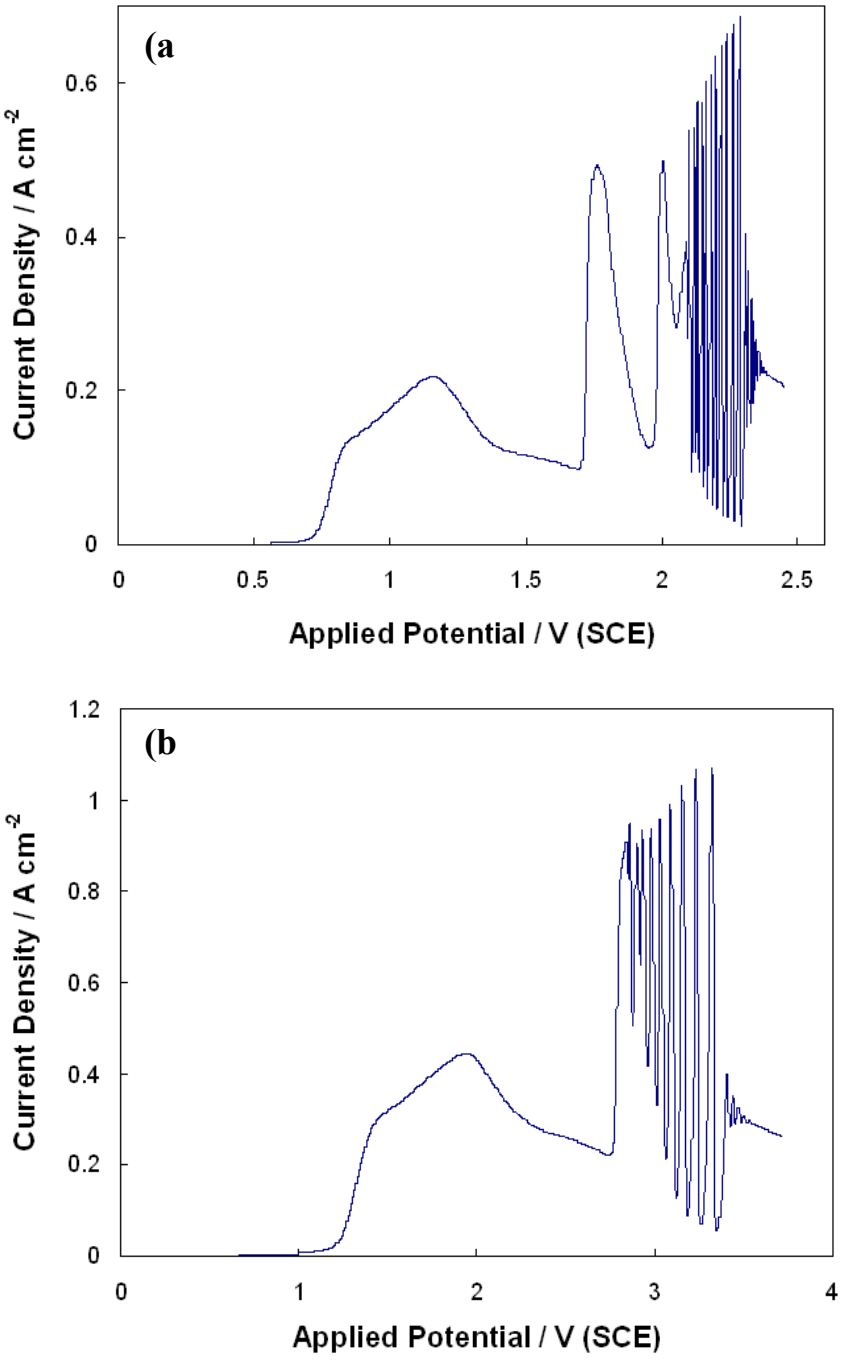

Fig. 1 Current density vs. potential curves of n-InP in 5 mol dm^{-3} KOH. The potential was scanned at (a) 100 mV s^{-1} from 0.0 V to 2.45 V and (b) 400 mV s^{-1} from 0.0 V to 3.7 V.

Fig. 2 shows, on an expanded potential axis, the current oscillations shown in Fig. 1a. The current density of each oscillation increases with a progressively increasing slope up to a well defined current maximum followed by a sharp decrease to a well defined current minimum.

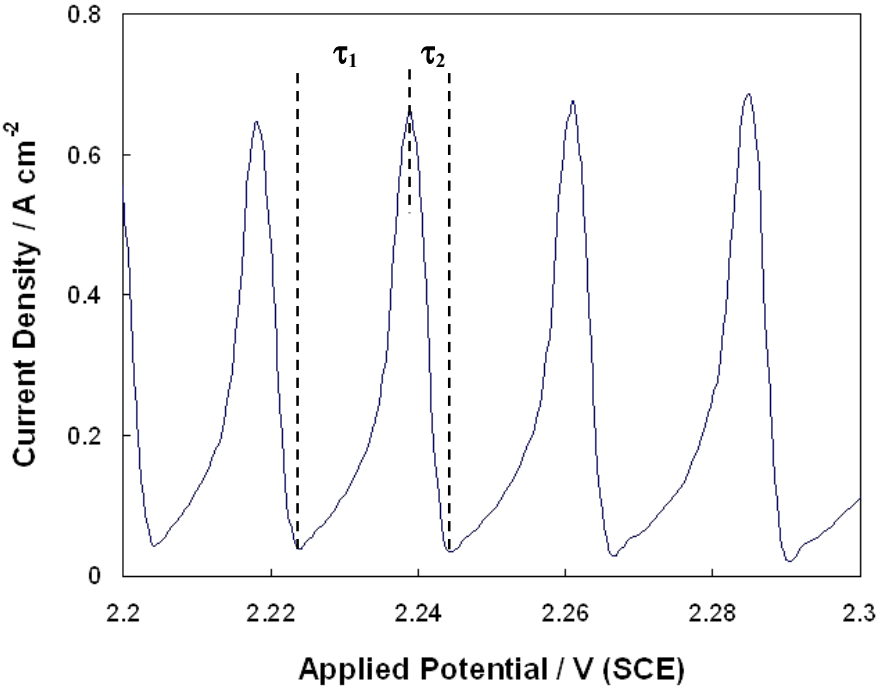

Fig. 2 Typical current oscillations observed during anodization of n-InP at a scan rate of 100 mV s^{-1} in 5 mol dm^{-3}. The potential axis has been expanded for clarity in the figure. The characteristic period segments τ_1 and τ_2 are shown.

The period segment τ_1 is defined to be the time taken for the current to increase from a minimum value to a maximum value during an oscillation. The period segment τ_2 is defined as the time taken for the current to decrease from a maximum to a minimum in current during an oscillation. The total period of oscillation is then $(\tau_1 + \tau_2)$. For the purposes of studying the potential dependence, we define the potential of an oscillation as the potential value at the current maximum for the oscillation.

The relationship of the values of τ_1, τ_2 and $(\tau_1 + \tau_2)$ to potential was investigated by plotting them against the applied potential. Data from Fig. 1 is plotted in this way in Fig. 3. The total period of oscillation $(\tau_1 + \tau_2)$ is observed to increase linearly at a rate of 0.906 s V^{-1} as the potential is increased. The value of τ_1 is also found to increase linearly with applied potential. However, the value of τ_2 decreases slightly at a rate of 0.096 s V^{-1} as the applied potential increases. From Fig. 3 it is apparent that the total period of oscillation, and indeed one of its constituent parts τ_1, show a well defined strong dependence on the value of the potential, whereas the value of τ_2 is much less sensitive to the value of the applied potential.

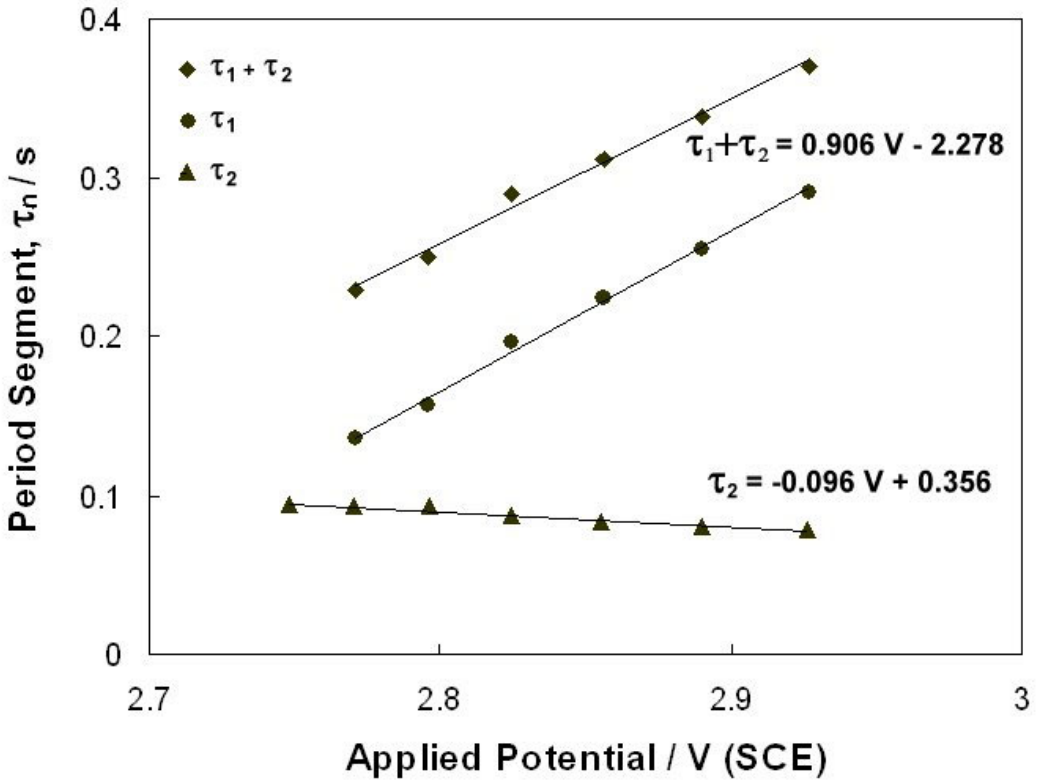

Fig. 3 Variation of τ_1, τ_2 and (τ_1 + τ_2) as a function of oscillation potential. The data was acquired from a linear potential sweep of n-InP in 5 mol dm^{-3} KOH at a scan rate of 100mV s^{-1} (as shown in Fig. 1a).

Investigation of the oscillatory region of linear potential sweeps obtained at scan rates in the range 50 mV s^{-1} to 500 mV s^{-1} revealed that the oscillation profile retains the same form as that shown in Fig. 2, regardless of the scan rate.

The charge passed during each oscillation was estimated by numerical integration of the current with respect to time. This was done for each oscillation in the potential sweep in Fig. 1 (i.e. same data set as Fig. 3). The charge per oscillation was plotted against the potential of the oscillation and a typical plot is shown in Fig. 4. The charge associated with the segments τ_1 and τ_2 are also plotted (Q_1 and Q_2 respectively). As can be seen in Fig. 4 the total charge per cycle (Q1 + Q_2) increases with increasing potential and a rate of approximately 0.268 C cm^{-2} V^{-1} was obtained from the slope of the linear fit to the data. The charge passed during the time segment τ_1 also increases linearly with increasing potential, whereas the charge passed during the time segment τ_2 decreases slightly as the potential increases. The segment, τ_1, is observed to represent the major portion of the total charge per cycle, whereas the charge associated with segment τ_2 is relatively constant with a measured decrease of 0.032 C cm^{-2} V^{-1}.

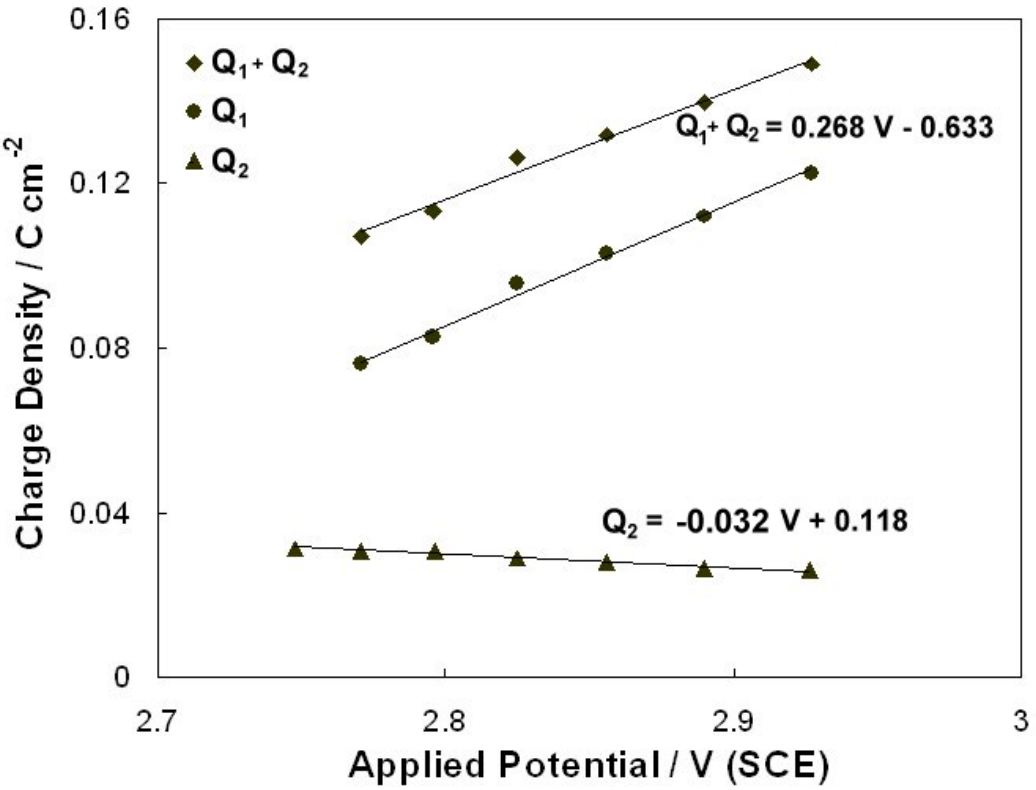

Fig. 4 Variation of the total charge per cycle ($Q_1 + Q_2$), charge associated with time τ_1 (Q_1) and charge associated with τ_2 (Q_2), as a function of potential. The data was acquired from a linear sweep of n-InP in 5 mol dm^{-3} KOH at a scan rate of 100 mV s^{-1} (as shown in Fig. 1a).

The charge per cycle was also estimated by numerical integration for the series of potential sweeps with scan rates in the range of 50 mV s^{-1} to 500 mV s^{-1}. This data was plotted as a function of the potential of oscillation and a linear dependence was observed as shown in Fig. 5. The slope of the linear fit yields a value of 0.216 C cm^{-2} V^{-1} for the increase in the charge per cycle with potential. It is noted that, as the scan rate increases, the range of the oscillatory region is shifted to higher potentials. The composite data set (represented in Fig. 5) therefore includes a larger overall range of potential and the charge per cycle is a well-behaved linear function of potential over this expanded range.

Fig. 6 shows a bright field through focal TEM image of a sample which was anodized from 0.0 V to 2.35 V at a scan rate of 100 mV s^{-1}. Three distinct layers can be observed on the surface of the InP: an obviously porous layer at C next to the substrate D, an intermediate layer B and an outer porous layer A. TEM electron diffraction has been used to identify layers A and C as InP, and layer B as In_2O_3.

Higher magnification TEM images reveal that the In_2O_3 layer appears to be porous and also suggests that the layer labeled C in Fig. 6 is a pitted region of the InP substrate. TEM images of electrodes anodized to 1.7 V at a scan rate of 100 mV s^{-1} (i.e. potential prior to the onset of oscillation) show only the InP substrate and a dense porous upper layer of InP corresponding to region A in Fig. 6. Thus, it appears that the pitting of the

substrate (C) and growth of the In_2O_3 film (B) occurs during the potential region in which oscillations are observed.

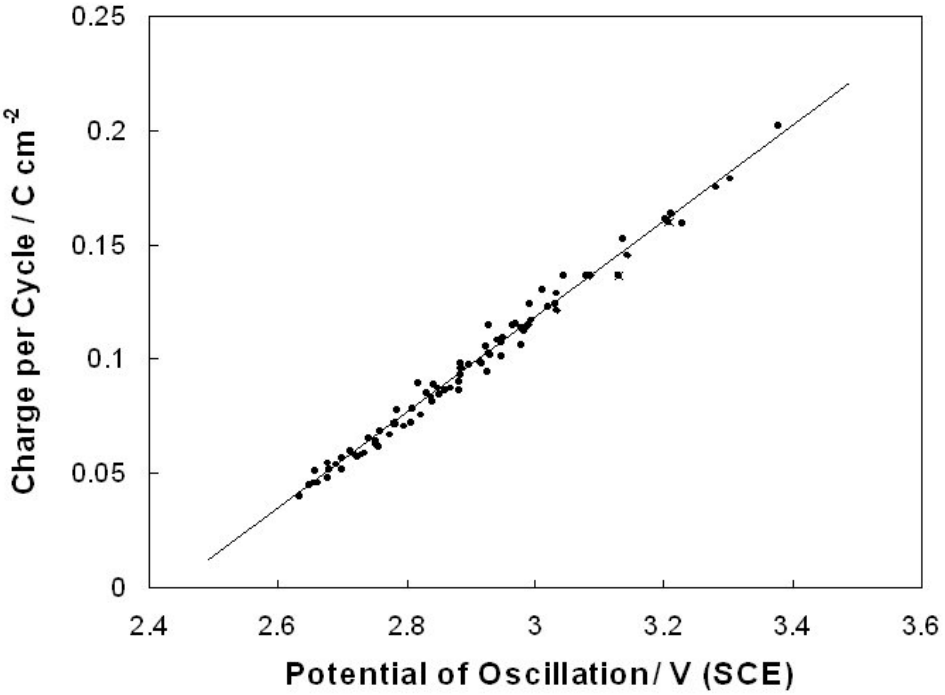

Fig. 5 Total charge per cycle plotted as a function of potential. The data was acquired from potential sweeps of n-InP in 5 mol dm^{-3} KOH with scan rates in the range 50 mV s^{-1} to 500 mV s^{-1}.

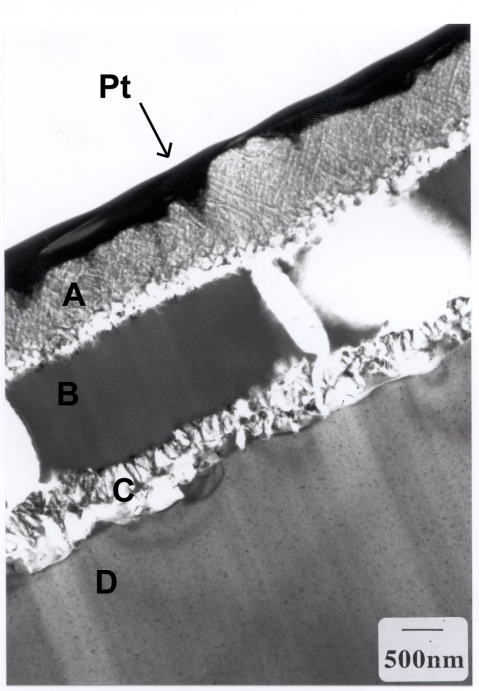

Fig. 6 Bright field through focal TEM of an n-InP electrode after anodization from 0.0 V to 2.35 V (SCE) in 5 mol dm^{-3} KOH at a rate of 100 mV s^{-1}. A Pt layer is indicated which was deposited to prevent ion image to the underlying material during the preparation of the TEM sample. Four distinct layers are marked at A, B, C and D.

InP/$(NH_4)_2S$

Current oscillations are also observed when n-InP electrodes are anodized in a 3 mol dm^{-3} $(NH_4)_2S$ solution. Fig. 7 shows the current density vs. potential characteristics during a linear potential sweep from 0.0 V to 2.4 V scanned at a rate of 10 mV s^{-1}. Pronounced oscillations are observed and appear when the potential is greater than 1.7 V. As is evident from Fig. 7, as the current increases, the frequency of the oscillation also increases. The measured period of the oscillation spans a range of 6.67 s to 3.13 s under these conditions. Further details of the oscillatory behavior of InP in $(NH_4)_2S$ can be found elsewhere [19,20,23].

Fig. 8 shows, on an expanded potential axis, the current oscillations shown in Fig. 7. It is obvious that oscillations observed under potential sweep conditions in the sulfide electrolyte have a fairly symmetrical waveform with a sinusoidal appearance and with $\tau_1 \cong \tau_2$ over the whole potential range. This contrasts sharply with the waveform observed in the KOH electrolyte.

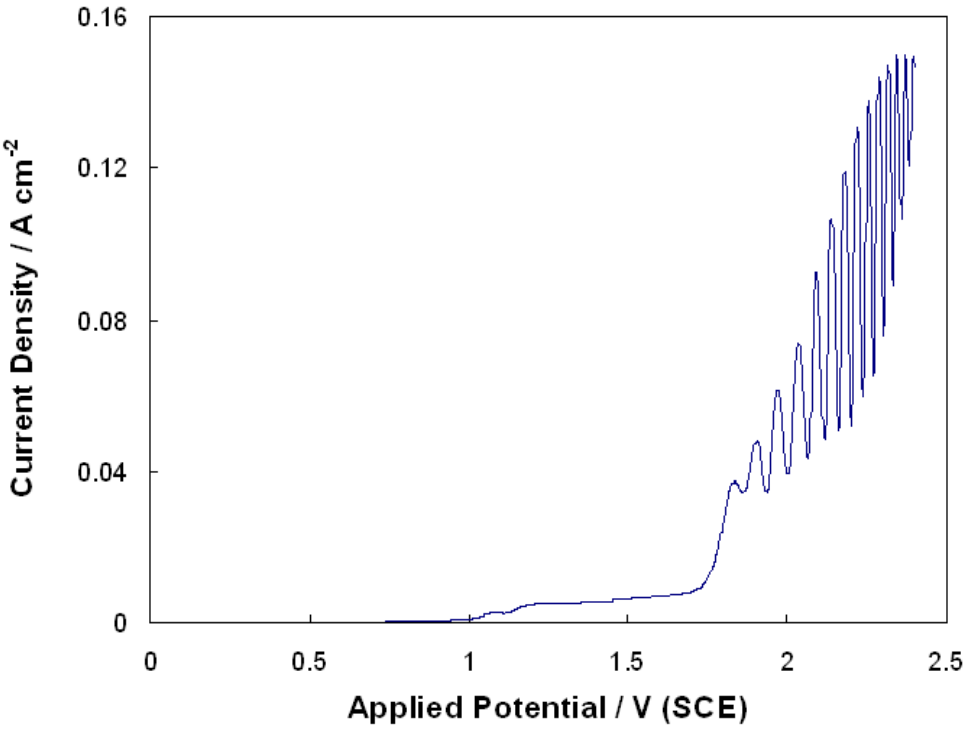

Fig. 7 Linear potential sweep of n-InP from 0.0 to 2.4 V (SCE) in a 3 mol dm^{-3} $(NH_4)_2S$ electrolyte at a scan rate of 10 mV s^{-1}. The oscillations are noted in the potential range 1.7 V to 2.4 V (SCE).

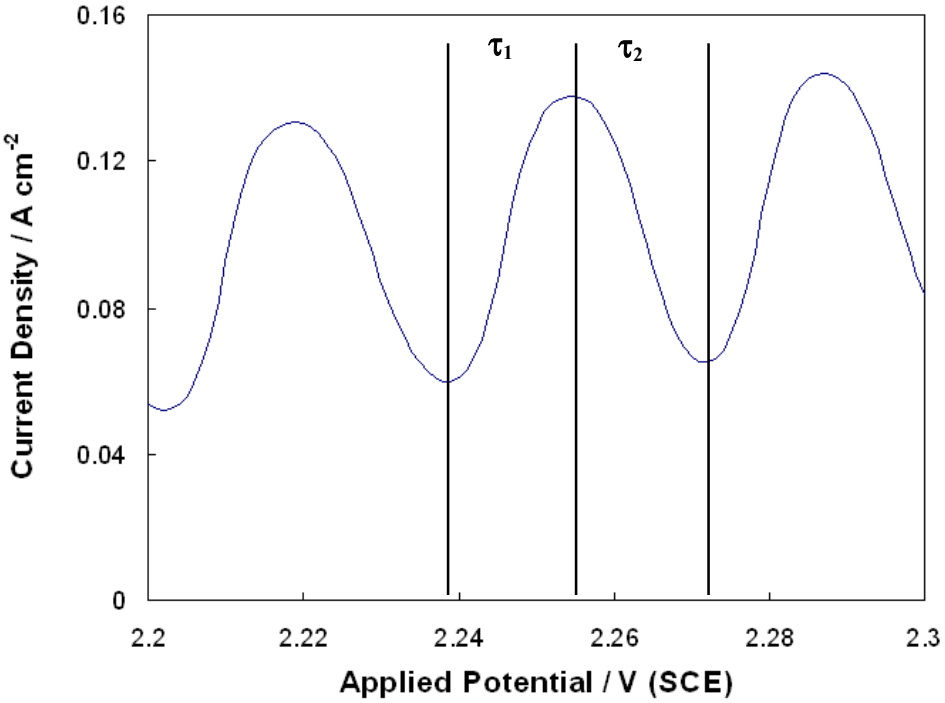

Fig. 8 Typical current oscillations observed during a linear potential sweep of n-InP in 3 mol dm^{-3} $(NH_4)_2S$ at a scan rate of 10 mV s^{-1}. The potential axis has been expanded for clarity in the figure. The characteristic period segments τ_1 and τ_2 are shown.

In Fig. 9 the charge per cycle, acquired from numerical integration of the current over time for InP electrodes anodized at various scan rates in 3 mol dm^{-3} $(NH_4)_2S$, is plotted as a function of the average potential of oscillation. Some variation is noted, but in general, the charge per cycle remains constant and has a value of 0.32 C cm^{-2}. Thus, as the potential increases in a potential sweep the current increases correspondingly and the charge per cycle remains constant, implying that the period of oscillation must decrease proportionately. Within the ranges studied, the charge per cycle remains constant irrespective of solution concentration, pH and scan rate for both potentiodynamic and potentiostatic anodization.

Microscopic examination of the electrodes after anodization show that the current oscillations observed during anodization in the $(NH_4)_2S$ solution are accompanied by the growth and thickening of a porous In_2S_3 film with columnar structure [24]. However, TEM images of samples anodized to 1.5 V (potential just prior to the onset of oscillations) show clearly defined pitting of the InP substrate with columnar film growth occurring from the bottom of the pits [22].

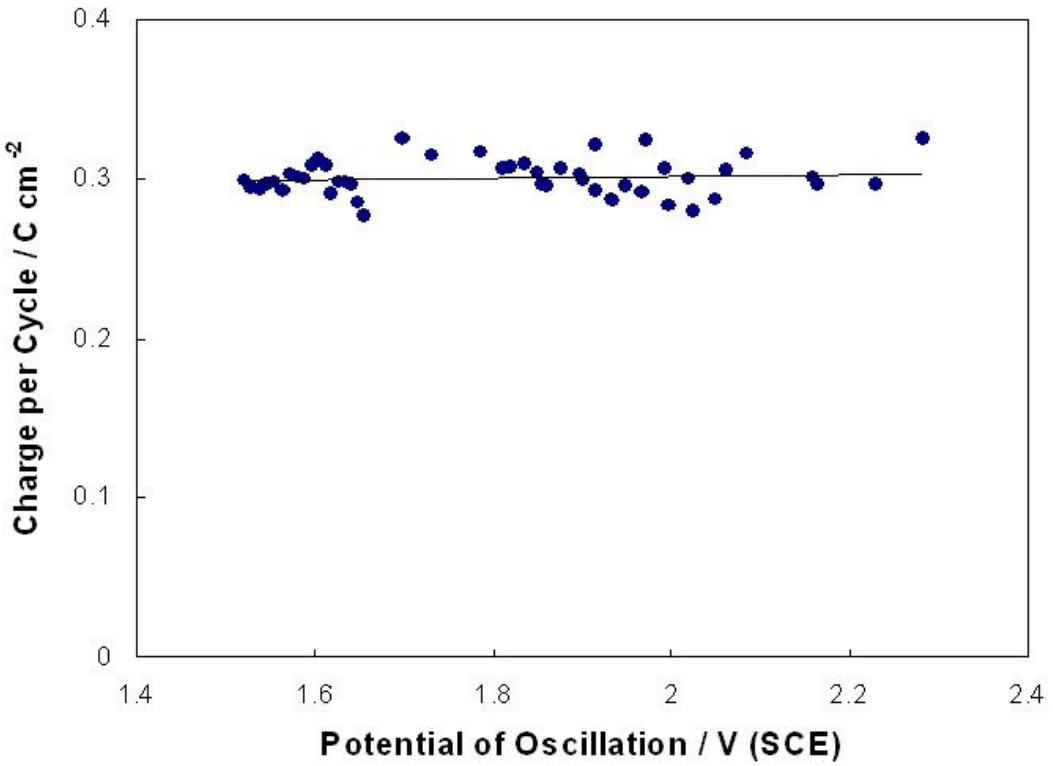

Fig. 9 Charge per cycle plotted as a function of potential for n-InP in 3 mol dm^{-3} $(NH_4)_2S$. The data was acquired from cyclic voltammograms at various scan rates. The charge was estimated by numerically integrating the current with respect to time.

CONCLUSIONS

Well defined oscillations are observed in both the InP/KOH and InP/$(NH_4)_2S$ systems. In the InP/ $(NH_4)_2S$ system oscillations observed have a fairly symmetric profile where $\tau_1 \cong \tau_2$ over the whole potential range. In contrast, the oscillations observed in the InP/KOH case exhibit an asymmetrical current vs. potential profile. The time segment τ_1 shows a clear dependence on the potential whereas the time segment τ_2 is almost independent of potential. The charge associated with segment τ_1 is observed to represent the major portion of the total charge per cycle and this increases with increasing potential. While the charge per cycle remains constant at 0.32 C cm^{-2} in the InP/$(NH_4)_2S$ irrespective of the value of the applied potential, in the InP/KOH system it is very clear that the charge per cycle increases linearly with potential. Thus, while the characteristics of the oscillations of the two systems investigated are dissimilar in many ways, both show reproducible and well-behaved values of charge per cycle. The exact mechanism of the oscillatory behavior is still under investigation. It may be related to the presence of a porous layer on the surface, since this is observed in both KOH and $(NH_4)_2S$ electrolytes and possibly involves periodic inhibition of processes at the electrode surface, due, either to cyclic electrolyte depletion or the anodic growth and dissolution of a passivating film at the interface.

REFERENCES

[1] P. Russell and J. Newman, *J. Electrochem. Soc.*, **133**, 2093 (1986)
[2] T.R. Beck, *J. Electrochem. Soc.*, **129**, 2412 (1982)
[3] D. Sazou, *Electrochim. Acta*, **42**, 627 (1997)
[4] S.H. Glarum and J.H. Marshall, *J. Electrochem. Soc.*, **132**, 2827 (1985)
[5] M.R. Bassett and J.L. Hudson, *J. Electrochem. Soc.*, **137**, 922 (1990)
[6] J.L. Husdon and T.T. Tsotsis, *Chem. Eng. Sci.*, **49**, 1493 (1994)
[7] D.J. Blackwood, A. Borazio, R. Greef, L.M. Peter and J. Stumper, *Electrochim. Acta*, **37**, 889 (1992)
[8] S. Cattarin, F. Decker and D. Dini, *J. Phys. Chem. B*, **102**, 4779 (1998)
[9] D. Dini, S. Cattarin and F. Decker, *J. Electroanal. Chem.*, **466**, 7 (1998)
[10] J.-N. Chazalviel, F. Ozanam, M. Etman, F. Paolucci, L.M. Peter and J. Stumper, *J. Electroanal. Chem.*, **327**, 343 (1992)
[11] M. Aggour, M. Giesig and H.J. Lewerenz, *J. Electroanal. Chem.*, **383**, 67 (1995)
[12] J. Carstensen, R. Prange and H. Föll, *J. Electrochem. Soc.*, **146**, 1134 (1999)
[13] S. Rauscher, Th. Dittrich, M. Aggour, J. Rappich, H. Flietner and H.J. Lewerenz, *Appl. Phys. Lett.,* **66**, 22 (1995)
[14] J. Stumper, R. Greef and L.M. Peter, *J. Electroanal. Chem.*, **310**, 445 (1991)
[15] V. Parkhutik, *Solid State Electron.*, **45**, 1451 (2001)
[16] V. Parkhutik, *Mater. Sci. Eng. B*, **88**, 269 (2002)
[17] H.J. Lewerenz and M. Aggour, *J. Electroanal. Chem.*, **351**, 159 (1993)
[18] V. Parkhutik, E. Matveeva, R. Perez, J. Alamo and D. Beltran, *Mater. Sci. Eng. B*, **69-70**, 553 (2000)
[19] E. Harvey and D.N. Buckley, *Electrochem. Solid-State Lett.*, **5**, G22 (2002)
[20] D.N. Buckley, E. Harvey and S.N.G. Chu, in *Proceedings of the State-of-the-Art Program on Compound Semiconductors XXXVI and Wide Bandgap Semiconductors for Photonic and Electronic Devices and Sensors III*, R.F. Kopf, F. Ren, E.B. Stokes, H.M. Ng, A.G. Baca, S.J. Pearton and S.N.G. Chu, Editors, PV 2002-3, p.286, The Electrochemical Society, Proceedings Series, Pennington, NJ (2002)
[21] S. Langa, J. Carstensen, I.M. Tiginyanu, M. Christophersen and H. Föll, *Electrochem. Solid-State Lett.*, **4**, G50 (2001)
[22] E. Harvey, C. O'Dwyer, T. Melly, D.N. Buckley, V.J. Cunnane, D. Sutton, S.B. Newcomb and S.N.G. Chu, *Proceedings of the 35th State-of-the-Art Program on Compound Semiconductors*, P.C. Chang, S.N.G. Chu, and D.N. Buckley, Editors, PV 2001-2, p. 87, The Electrochemical Society, Proceedings Series, Pennington, NJ (2001)
[23] D.N. Buckley, E. Harvey and S.N.G. Chu, *Chemical Monthly*, **133**, 785 (2002)
[24] E. Harvey, D.N. Buckley, S.N.G. Chu, D. Dutton and S.B. Newcomb, *J. Electrochem. Soc.*, **149** (Sept. 2002)